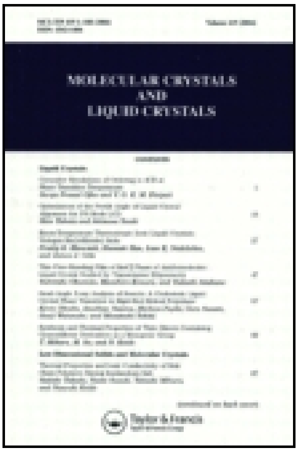

Molecular Crystals and Liquid Crystals
Publication details, including instructions for authors and subscription information:
http://www.tandfonline.com/loi/gmcl20

Enhancement Mechanisms of the Color Purity in Blue Organic Light-Emitting Devices Fabricated Utilizing an Emitting Layer Containing Mixed Fluorescence and Phosphorescence Host Materials

H. S. Bang [a], D. C. Choo [a], T. W. Kim [a], S. J. Lee [b], J. H. Seo [b] & Y. K. Kim [b]

[a] Department of Electronics and Computer Engineering, Hanyang University, Seoul, 133-791, Korea

[b] Department of Information Display Engineering, Center for Organic Materials & Information Display (COMID), Hong-ik University, Seoul, 121-791, Korea

To cite this article: H. S. Bang, D. C. Choo, T. W. Kim, S. J. Lee, J. H. Seo & Y. K. Kim (2011): Enhancement Mechanisms of the Color Purity in Blue Organic Light-Emitting Devices Fabricated Utilizing an Emitting Layer Containing Mixed Fluorescence and Phosphorescence Host Materials, Molecular Crystals and Liquid Crystals, 551:1, 33-39

To link to this article: http://dx.doi.org/10.1080/15421406.2011.600127

Mol. Cryst. Liq. Cryst., Vol. 551: pp. 33–39, 2011

ISSN: 1542-1406 print/1563-5287 online
DOI: 10.1080/15421406.2011.600127

Enhancement Mechanisms of the Color Purity in Blue Organic Light-Emitting Devices Fabricated Utilizing an Emitting Layer Containing Mixed Fluorescence and Phosphorescence Host Materials

H. S. BANG,[1] D. C. CHOO,[1] T. W. KIM,[1,*] S. J. LEE,[2]
J. H. SEO,[2] AND Y. K. KIM[2]

[1]Department of Electronics and Computer Engineering, Hanyang University, Seoul 133-791, Korea
[2]Department of Information Display Engineering, Center for Organic Materials & Information Display (COMID), Hong-ik University, Seoul 121-791, Korea

The electrical and optical properties of blue organic light-emitting devices (OLEDs) containing a mixed host emitting layer (EML) consisting of a 1,3-bis(carbazole-9-yl)benzene (mCP) layer and a 3-tert-butyl-9,10-di(naphtha-2-yl)anthracene (TBADN) layer were investigated. The driving voltage of the OLEDs with a mixed host EML was smaller than that of the OLEDs with a single EML. The electroluminescence spectra for OLEDs containing a mixed host EML showed a dominant peak related to the mCP or the TBADN layer. The color coordinates of the OLEDs containing a 5% TBADN-doped mCP EML were (0.146, 0.091), indicative of the deep blue color coordinates.

Keywords Blue organic light-emitting devices; color purity; mixed host emitting layer; driving voltage; electroluminescence; color coordinates

Introduction

Organic light-emitting devices (OLEDs) have been particularly attractive due to interest in their promising applications in full-color flat-panel displays [1–5]. OLED displays have been currently receiving considerable attention because of their potential applications in lighting sources and flexible displays, which offer unique advantages of low driving voltage, low power consumption, high contrast, wide viewing angle, high flexibility, low cost, and fast response [6, 7]. The prospect of potential applications of high-efficiency blue OLEDs has led to substantial research and development efforts to fabricate OLEDs with various kinds of unique structures [8]. However, blue OLEDs still have inherent problems of low efficiency, poor color purity, and short lifetime in comparison with red or green OLEDs [9]. OLEDs with various structures have been suggested for enhancing the efficiency and the color stability of blue OLEDs [10–14]. Even though some works on the efficiency enhancement in green or white OLEDs with a multiple emitting layer (EML) have been performed to improve the balance of holes and electrons in an EML [15–17], very few

---

*Corresponding author. E-mail: twk@hanyang.ac.kr

studies concerning the efficiency enhancement and the color purity in blue OLEDs utilizing a mixed host EML have been reported because of complicated device fabrication processes. Even though studies on the improvement of the luminance for the OLEDs with a fluorescence mixed host EML have been performed [18], very few investigations about the optical properties of OLEDs with a fluorescence and phosphorescence mixed host EML have been conducted [19, 20].

This paper reports data for the enhancement mechanisms of color purity in blue OLEDs with a mixed host EML deposited by using organic thermal evaporation. Current density-voltage, luminance-voltage, and luminance efficiencies-current density measurements were performed to investigate the efficiency enhancement and the color stabilization of the OLEDs with a mixed host EML consisting of a 1,3-bis(carbazole-9-yl)benzene (mCP) layer, a 3-tert-butyl-9,10-di(naphtha-2-yl)anthracene (TBADN) layer, or a mixed layer of mCP and TBADN acting as a mixed host EML. Electroluminescence (EL) measurements were carried out to investigate the energy transfer mechanisms of OLEDs containing mixed host EML layers with and without dopants. The Commission Internationale de l'Eclairage (CIE) chromaticity coordinates corresponding to the emission colors were determined to investigate the color purity of the OLEDs with a mixed host EML.

Experimental

The sheet resistivity of the indium-tin-oxide (ITO) thin films coated glass substrates used in this study was 15 Ω/square. The ITO coated glass substrates were cleaned using ultrasonic cleaning methods in acetone, methanol, and distilled water at 60°C for 15 min, and were rinsed in de-ionized water thoroughly. The chemically cleaned ITO substrates were kept for 48 h in isopropyl alcohol to remove totally residual impurities on the ITO surfaces. After the immersion process, the surface properties of the workfunction and surface resistance for the ITO films are not changed. After the chemically cleaned ITO substrates had been dried by using N_2 gas with a purity of 99.9999%, the surfaces of the ITO substrates were treated with an oxygen plasma for 2 min at an O_2 pressure of approximately 2×10^{-2} Torr. Five kinds of samples used in this study were deposited on ITO coated glass substrates by using organic thermal evaporation and consisted of the following structures from top: an aluminum (Al) (100 nm) cathode electrode, a lithium quinolate (Liq) (2 nm) electron injection layer (EIL), a 4,7-duphenyl-1,10-phenanthorolene (BPhen) (20 nm) electron transport layer (ETL), a 2,9-dimethyl-4,7-diphenyl-1,10-phenanthroline (BCP) (10 nm) hole blocking layer (HBL), five kinds of EMLs (30 nm), a N,N′-bis(naphthalene-1-yl)-N,N′-bis(phenyl)-9,9-spiro-bifluorene (Spiro-NPB) (50 nm) HTL, an ITO anode electrode, and a glass substrate. The EMLs used in this study consisted of an mCP (30 nm) layer, a TBADN (30 nm) layer, a 5% TBADN-doped mCP (30 nm) layer, a 20% TBADN-doped mCP (30 nm) layer, or a 50% TBADN doped mCP (30 nm) layer, which are denoted by devices I, II, III, IV, and V. The device structures are summarized in Table 1. After organic and metal layers were deposited on the ITO thin films coated on glass substrates, the OLED devices were covered by using a glass cap and sealed by using epoxy in a glove box with O_2 and H_2O concentrations below 1 ppm. A desiccant material consisting of a barium-oxide powder was used to absorb the residual moisture and oxygen in the encapsulated device. The deposition rates of the organic layers and the metal layers were approximately 0.1 and 0.15 nm/s, respectively, and the deposition rates were controlled by using a quartz crystal monitor. The emitting area in the pixel was 3 mm × 3 mm. The current density-voltage characteristics of the OLEDs were measured on a programmable electrometer with built-in current and voltage measurement units (model SMU-236, Keithely). The brightness was measured by using

Table 1. Device structures of the blue OLEDs with a mixed host EML.

	Anode	HTL	EML	HBL	ETL	Cathode
Device I	ITO (100 nm)	Spiro-NPB (50 nm)	mCP (30 nm)	BCP (10 nm)	BPhen (20 nm)	Al (100 nm)
Device II			TBADN (30 nm)			
Device III			5% TBADN doped mCP (30 nm)			
Device IV			20% TBADN doped mCP (30 nm)			
Device V			50% TBADN doped mCP (30 nm)			

a brightness meter, chromameter CS-100A (Minolta). The EL spectra were measured by using a spectrometer (Perkin-Elmer LS20B instruments).

Results and Discussion

Figure 1 shows the current densities as functions of the applied voltage for devices I, II, III, IV, and V. Opened squares and circles represent the data for devices I and II containing undoped EMLs, respectively. Filled squares, circles, and triangles represent the data for devices III, IV, and V containing an mCP EML with a TBADN doping concentration of 5, 20, or 50%, respectively. The highest occupied molecular orbital (HOMO) and the lowest unoccupied molecular orbital (LUMO) levels of the mCP molecule are −6.1 and −2.4 eV, as determined by cyclic voltametry, respectively. The HOMO and LUMO levels of the TBADN molecule are −5.7 and −3.0, respectively. The electron mobility of device II with a TBADN EML is larger than that of device I with an mCP EML because the triplet levels of the mCP molecule is relatively high, resulting in an increase in the turn-on voltage of device I. While the current density of device III containing an mCP EML with a TBADN doping concentration of 5% is almost the same as that of device I with an mCP EML,

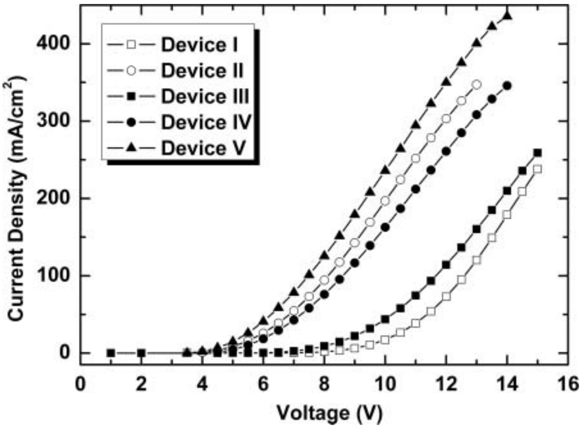

Figure 1. Current densities as functions of the applied voltage of devices I, II, III, IV, and V. Opened squares and circles and filled squares, circles, and triangles represent data for devices I, II, III, IV, and V, respectively.

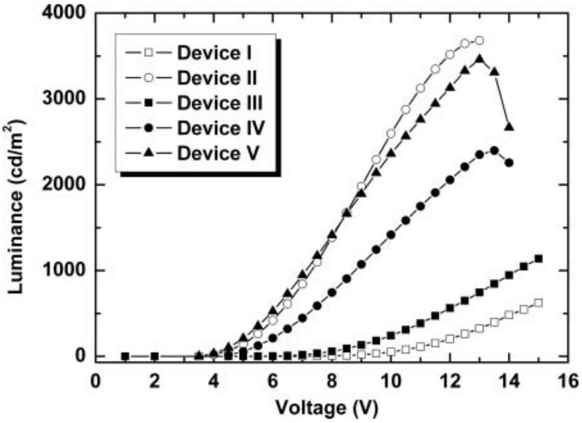

Figure 2. Luminances as functions of the applied voltage of devices I, II, III, IV, and V. Opened squares and circles and filled squares, circles, and triangles represent data for devices I, II, III, IV, and V, respectively.

the current density of device IV is almost the same as that of device II with a TBADN EML, resulting that an increase in the doping concentration of the TBADN enhances the current density of device IV. However, the current density of device V containing an mCP EML with a TBADN doping concentration of 50% is larger than that of device II because of an increase in electrons and holes, which do not contribute to the emission process.

Figure 2 shows the luminances as functions of the applied voltage for devices I, II, III, IV, and V. Opened squares and circles represent devices I and II containing undoped EMLs, respectively. Filled squares, circles, and triangles represent the data for devices III, IV, and V containing an mCP EML with a TBADN doping concentration of 5, 20, or 50%, respectively. The trend of the luminescence-voltage characteristics for all devices is almost similar to that of the current density-voltage characteristics. However, the current density of device V increases more than device II due to an increase of the trap sites for electrons and holes resulting from the mismatch of energy levels between the TBADN and the mCP molecules. The luminance of device II is larger than that of device V because the TBADN molecules are fluorescent materials with a high radiative rate. The luminance of the OLEDs with a TBADN-doped EML increases with increasing doping concentration of the TBADN due to an increase in the energy transfer of the exciton from the mCP molecule to the TBADN molecule.

Figure 3 shows the luminance efficiencies as functions of the current density for devices I, II, III, IV, and V. While the luminance efficiency of device II has the highest value among the devices, the luminance efficiency of device I has the lowest value among the devices. Even though the luminance efficiency-current density curves are almost similar to the current density-voltage curves and the luminance-voltage curves, the luminance efficiency of device V is lower than that of device II. Because the current density of device V is larger than those of the other devices, the luminance efficiency of device V is lower than that of device II.

The CIE coordinates at 14 V of devices I, II, III, IV, and V with different TBADN concentrations are shown in Fig. 4. While the CIE coordinates of device III containing an mCP EML with a TBADN doping concentration of 5% are (0.146, 0.091), which are the closest value to the national television standard committee (NTSC) blue coordinates of (0.14, 0.09), those of devices III and IV are (0.157, 0.138) and (0.156, 0.174), which

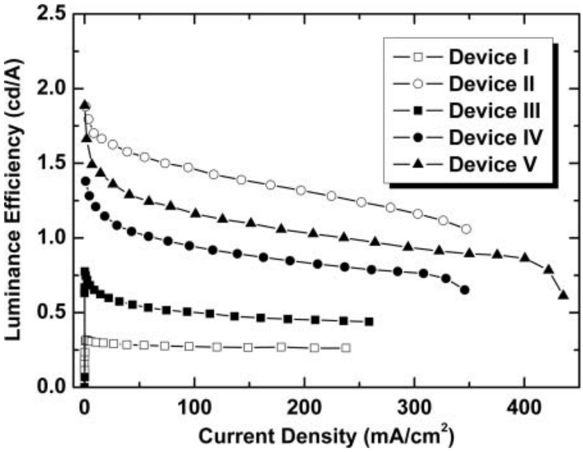

Figure 3. Luminance efficiencies as functions of the current density for devices I, II, III, IV, and V. Opened squares and circles and filled squares, circles, and triangles represent devices I, II, III, IV, and V, respectively.

are far from the NTSC blue color. Because the exciton energy transfer from the mCP phosphorescence host molecules to the TBADN fluorescence host molecules increases through the Förster energy transfer process, the CIE coordinates of the OLEDs with a mixed host EML are the closest value to the NTSC blue color coordinates.

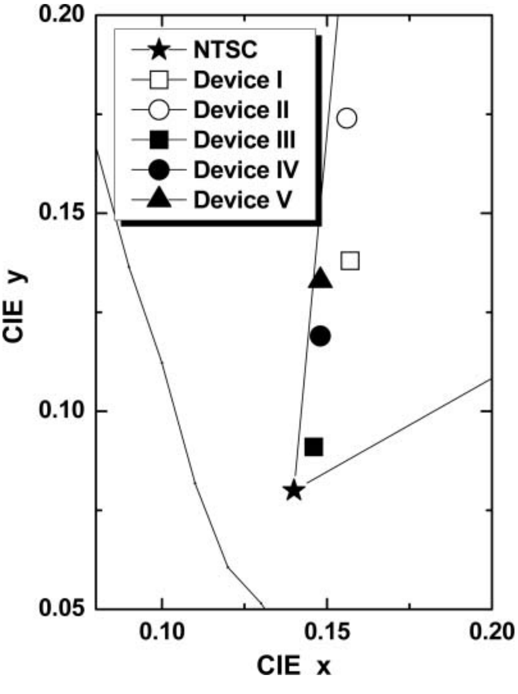

Figure 4. Commission Internationale de l'Eclairage (CIE) chromaticity coordinates at 14 V for devices with different concentrations. Filled rectangles represent CIE x coordinates and empty circles represent CIE y coordinates.

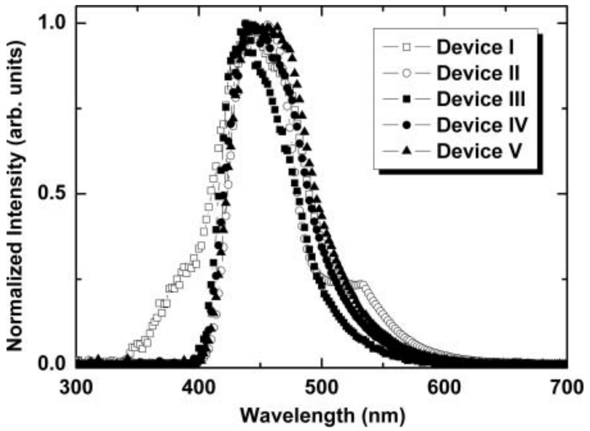

Figure 5. Electroluminescence spectra at 14 V for devices I, II, III, IV, and V. Opened squares and circles and filled squares, circles, and triangles represent data for devices I, II, III, IV, and V, respectively.

The EL spectra at 14 V for devices I, II, III, IV, and V are shown in Fig. 5. The dominant EL peaks at 14 V for blue OLEDs with an mCP EML or a TBADN EML are located at 438 and 442 nm, respectively. When the mCP and the TBADN are used as phosphorescence and fluorescence host materials, respectively, the excitons are transferred from the host molecules to the dopant molecules through the Förster energy transfer process or Dexter energy transfer process. However, the excitons existing in the phosphorescence host molecules of the mCP in OLEDs with a mixed host EML are transferred into the fluorescence host molecules of TBADN through the Förster energy transfer process, resulting in the shift of dominant EL peaks toward shorter wavelength and a decrease in full widths at half maximum (FWHM) of the EL spectra of the OLEDs with a mixed host EML.

Conclusions

The enhancement mechanisms of color purity in blue OLEDs fabricated utilizing mixed host EMLs was investigated. The driving voltage of the OLED containing an mCP EML with a TBADN doping concentration of 5% was smaller than that of the OLEDs with an mCP single EML. The color coordinates of the OLED containing an mCP EML with a TBADN doping concentration of 5% were almost the same value as the blue color of NTSC coordinates because the exciton transfer probability from the TBADN to the mCP was the highest value. The FWHM of the EL spectra for the OLEDs containing the TBADN doped mCP EML was very small, and the dominant EL peak was shifted to shorter wavelength side. These results can help improve understanding of the enhancement mechanisms of color purity in blue OLEDs with a mixed host EML.

Acknowledgment

This work was supported by the National Research Foundation of Korea (NRF) grant funded by the Korea government (MEST) (No. 2010-0018877).

References

[1] Tang. C. W., Van Slyke. S. A., *Appl. Phys. Lett.*, **51**, 913, (1987).

[2] Baldo, M. A., O'Brien, D. F., You, Y., Shoustikov, A., Sibley, S., Thompson, M. E., Forrest, S. R., *Nature*, **395**, 151, (1998).

[3] Friend, R. H., Gymer, R. W., Holmes, A. B., Burroughes, J. H., Marks, R. Taliani, N., C., Bradley, D. D. C., Dos Santos, D. A., Bredas, J. L., Löglund, M., Salaneck, W. R., *Nature*, **397**, 121, (1999).

[4] Aziz, H., Popovic, Z. D., Hu, N-X., Hor, A-M., Xu, G., *Science*, **283**, 1900, (1999).

[5] Baldo, M. A., Thompson, M. E., Forrest, S. R., *Nature*, **403**, 750,(2000).

[6] Adachi, C., Baldo, M. A., Forrest, S. R., Lamansky, S., Thompson, M. E., Wong, R. C., *Appl. Phys. Lett.*, **78**, 1622, (2001).

[7] Fukuda, Y., Watanabe, T., Wakimoto, T., Miyaguchi, S., Tsuchida, M., *Synth. Met.*, **111–112**, 1, (2000).

[8] Holmes, R. J., Forrest, S. R., Sajoto, T., Tamayo, A., Djurovich, P. I., Thompson, M. E., Brooks, J., Tung, Y. J., D'Andrade, B. W., Weaver, M. S., Kwong, R. C., Brown, J. J., *Appl. Phys. Lett.*, **87**, 243507, (2005).

[9] Li, G., Shinar, J., *Appl. Phys. Lett.*, **83**, 5359, (2003).

[10] Liu, S. W., Huang, C. A., Yang, J. H., Chen, C. C., Chang, Y., *Thin Solid Films*, **453–454**, 312, (2004).

[11] Lu, H. T., Tsou, C. C., Yokoyama, M., *J. Cryst. Growth*, **277**, 388, (2005).

[12] Zou, L., Savvate'ev, V., Booher, J., Kim, C. H., Shinar, J., *Appl. Phys. Lett.*, **79**, 2282, (2001).

[13] Im, W. B., Hwang, H. K., Lee, J. G., Han, K. J., Kim, Y. K., *Appl. Phys. Lett.*, **79**, 1387, (2001).

[14] Chen, B., Zhang, X. H., Lin, X. Q., Kwong, H. L., Wong, N. B., Lee, C. S., Gambling, W. A., Lee, S. T., *Synth. Met.*, **118**, 193, (2001).

[15] Huang, J., Yang, K., Xie, Z., Chen, B., Jiang, H., Liu, S., *Appl. Phys. Lett.*, **73**, 3348, (1998).

[16] Fujita, S., Nakazawa, T., Asano, M., Fujita, S., *Jpn. J. Appl. Phys.*, **39**, 5301, (2000).

[17] Qiu, Y., Gao, Y., Wang, L., Wei, P., Duan, L., Zhang, D., Dong, G., *Appl. Phys. Lett.*, **81**, 3540, (2002).

[18] Hamada, Y., Kanno, H., Tsujioka, T., Takahashi, H., Usuki, T., *Appl. Phys. Lett.* **75**, 1682, (1999).

[19] Lee. J. H., Wu. C. H., Liu. S. W., Huang. C. A., Chang. Y., *Appl. Phys. Lett.* **86**, 130506, (2005).

[20] Joo. C. W., Jeon. S. O., Yook. K. S., Lee. J. Y., *Org. Electron.* **11**, 36 (2010).